

# Weakest-link Failure Prediction for Ceramics IV: Application of Mixed-mode Fracture Criteria for Multiaxial Loading

L. Dortmans & G. de With\*

Centre for Technical Ceramics, P.O. Box 595, 5600 AN Eindhoven, The Netherlands

(Received 22 July 1991; revised version received 4 November 1991; accepted 7 November 1991)

## Abstract

Strength data obtained from uniaxial and biaxial bend tests on two alumina ceramics have been analysed by means of a weakest-link model with different mixed-mode fracture criteria and crack shapes. Taking the data from three- and four-point bend tests as a reference, strength predictions for the ball-on-ring and ring-on-ring biaxial tests were made, showing large differences in the predictions for the different fracture criteria. The best fitting models for the two aluminas cannot be interchanged, thus showing a marked difference in their shear stress sensitivity. Analysis shows that in general a combination of tests with a varying degree of stress multiaxiality is required to determine the best applicable mixed-mode fracture criterion.

Es wurden Festigkeitsdaten, die mit Hilfe uniaxialer und biaxialer Biegeversuche an zwei Aluminiumoxid-Keramiken gewonnen wurden, mittels eines Modells für schwächste Verbindungsstellen analysiert, wobei verschiedene Bruchkriterien für überlagerte Belastungsmoden und verschiedene Rißgeometrien berücksichtigt wurden. Die Daten aus den Drei- und Vier-Punkt-Biegeversuchen wurden als Bezugsquelle gewählt, um Festigkeitsvorhersagen für den Kugel-auf-Ring-Biegeversuch und für den Ring-auf-Ring-Biegeversuch durchzuführen. Es stellte sich hierbei heraus, daß große Unterschiede in der Vorhersage für die verschiedenen Bruchkriterien existieren. Die besten Modelle für die zwei Aluminiumoxid-Keramiken können nicht ausgetauscht werden, was den deutlichen Unterschied in ihrer Empfindlichkeit auf Scherspannungen widerspiegelt. Die Analyse

\* Also affiliated with Philips Research Laboratories, P.O. Box 80000, 5600 JA Eindhoven, The Netherlands.

zeigt, daß im allgemeinen eine Kombination verschiedener Versuche mit einem variierenden Grad der Spannungs-Vielachsigkeit erforderlich ist, um das beste Bruchkriterium für überlagerte Belastungsmoden zu bestimmen.

Des données sur la résistance mécanique obtenues à partir d'essais uniaxiales et biaxiales de flexion sur deux céramiques à base d'alumine ont été analysées par rapport au modèle de rupture du maillon le plus faible avec différents critères de mode de fracture et différentes formes de fissures. En prenant les données des tests de flexion trois et quatre points comme référence, des prédictions sur la résistance mécanique pour les essais biaxiales bille sur anneau et anneau sur anneau ont été faites, qui montrent de grandes différences dans les prédictions pour les différents critères de fracture. Les modèles le plus adapté pour les deux aluminas ne peuvent pas être interchangé, car elles présentent une différence marquée dans leurs contraintes de cisaillement. Les analyses montrent qu'en générale la combinaison de plusieurs tests avec un degrés variable de contrainte multiaxiale est nécessaire pour déterminer le critère de mode de fracture le plus applicable.

## 1 Introduction

Failure probability prediction for brittle ceramics in a multiaxial stress state has been addressed in the literature on a number of occasions. Generally, an extended weakest-link model is applied in conjunction with a suitable mixed-mode fracture criterion.<sup>1–3</sup> This fracture criterion, indicating the start of unstable crack growth, can be derived by applying linear elastic fracture mechanics (LEFM) to a plane

crack subjected to both normal and shear stresses. Several of these criteria have been proposed and applied to experimental results, which frequently consist of strength data obtained from uniaxial or biaxial flexure tests.<sup>1,4-7</sup> So far it has not been established whether a generally valid fracture criterion exists. It may well be possible that such a fracture criterion does not exist, due to large differences in microstructure and flaw populations encountered in ceramics. Apart from this it has also been argued that flexure tests may not provide sufficient information to determine whether a particular fracture criterion is valid, because simultaneous positive and negative principal stresses are not sufficiently present.<sup>1</sup> To the authors' knowledge explicit proof for this statement has not been given in detail. In the present analysis experimental results for two types of alumina are considered, which have been reported earlier.<sup>4</sup> Several flexure tests were carried out on these materials to obtain uniaxial and biaxial strength data. The first objective of this paper is to indicate which fracture criterion is best suited for these materials. Once this has been established it will be discussed whether alternative tests can provide a better discrimination between the different fracture criteria considered.

## 2 Modelling and Experimental Results

The failure probability relation for surface defects can be formulated as

$$P_f = 1 - \exp \left[ - \left( \frac{1}{m!} \right)^m \left( \frac{S_{\text{nom}}}{\bar{S}_{\text{nom}}} \right)^m \right] \quad (1)$$

$$\bar{S} = S_u \left( \frac{A_u}{A \Sigma(A)} \right)^{1/m} \quad (2)$$

$$\Sigma(A) = \frac{1}{A} \int_A \left[ \frac{1}{2\pi} \int_{C_u} \left( \frac{\sigma_{\text{eq}}}{S_{\text{nom}}} \right)^m dC_u \right] dA \quad (3)$$

with  $m$  as the Weibull modulus,  $(1/m!) = \Gamma[1 + (1/m)]$ ,  $S_{\text{nom}}$  as a nominal or reference fracture stress,  $\bar{S}_{\text{nom}}$  as the mean nominal fracture stress,  $A_u = 1$  as a unit surface,  $S_u$  as the unit strength,  $A$  as the surface of the component,  $\Sigma(A)$  as the stress surface integral,  $C_u$  as the contour of a circle with unit radius and  $\sigma_{\text{eq}}$  as the equivalent fracture stress. The expressions given above are the result of combining the four-parameter notation introduced by Stanley *et al.*<sup>8</sup> and the fracture model proposed by Batdorf and coworkers.<sup>2,3</sup> Along the lines and formulae given in the Appendix,  $\sigma_{\text{eq}}$  can be determined from several available mixed-mode

**Table 1.** Experimental results for two aluminas (Wesgo 997 and NKA-cip) taken from Ref. 4

Material A: Wesgo		Material B: NKA
Weibull modulus $m = 22.1$	Weibull modulus $m = 8.0$	Weibull modulus $m = 8.0$
Test	$\bar{S}_{\text{nom}}$ (MPa)	$\bar{S}_{\text{nom}}$ (MPa)
3P20	288.9	371.2
3P40	280.4	
4P40	263.8	298.8
BOR	287.7	
ROR	229.8	263.7

$\bar{S}_{\text{nom}}$  = Mean fracture stress from fit procedure; 3P20 = three-point bending with 20 mm support; 3P40 = three-point bending with 40 mm support; 4P40 = four-point bending with 20 mm span and 40 mm support; BOR = ball-on-ring; ROR = ring-on-ring.

fracture criteria. The fracture criteria considered in this paper are:

- PIA: principal of independent action<sup>8</sup>
- NSA: normal stress averaging or mode I failure
- COP: coplanar energy release rate<sup>9</sup>
- GMAX: maximum noncoplanar energy release rate<sup>10</sup>
- RNC: empirical criterion of Richard<sup>11</sup>

As indicated by Thiemeier *et al.*,<sup>1</sup> GMAX, COP and RNC can be applied to through-the-thickness (TTC) or penny-shaped cracks (PSC), while for RNC the parameter  $\alpha$  has to be specified as well (see the Appendix). For numerical calculations use has been made of the finite element post-processor FAILUR which incorporates the failure criteria mentioned.<sup>12</sup>

The experimental results for the two materials considered have been given in a previous paper<sup>4</sup> and are summarized in Table 1.

## 3 Analysis of Results for Three- and Four-point Bend Tests

The results obtained for the three- and four-point bend tests can be used to determine the value for the yet unknown unit strength  $S_u$  for the various models and materials. This value will then be used to predict the biaxial strength for ball-on-ring (BOR) and ring-on-ring (ROR), such that a comparison between predicted and measured values can be made to see which fracture criterion fits best. Using the post-processor FAILUR after a finite element analysis,  $S_u$  can be determined for 3P20, 3P40 and 4P40 such that the predicted value  $\bar{S}_{\text{nom}}^{\text{pred}}$  for the mean fracture stress meets the measured values  $\bar{S}_{\text{nom}}$ . The results for the various materials, tests and models are given in Table 2. Ideally the value for  $S_u$  should be independent of the test considered. The results in

**Table 2.** Calculated and averaged values for the unit strength  $S_u$  (MPa) for materials A and B from the results of three- and four-point bend tests

Model	Material A: Wesgo				Material B: NKA			
	3P20	3P40	4P40	Mean	3P20	4P40	Mean	
PIA	315.9	312.1	322.2	316.7	512.9	525.3	519.1	
GMAX	TTC	306.1	302.5	312.3	307.0	468.4	479.7	474.0
GMAX	PSC	314.2	310.4	320.5	315.0	483.3	494.9	489.1
NSA		284.8	281.5	290.5	285.6	418.3	428.4	423.4
COP	TTC	291.1	287.6	296.9	291.9	436.2	446.7	441.5
COP	PSC	293.3	289.8	299.2	294.1	442.8	453.5	448.2
RNC $\alpha = 1.0$	TTC	298.7	295.2	304.7	299.5	455.3	466.3	460.8
	PSC	304.5	300.9	310.6	305.3	468.3	479.6	474.0
	$\alpha = 1.1$ TTC	302.8	299.2	308.9	303.6	464.8	476.0	470.4
	PSC	311.0	307.3	317.2	311.8	481.2	492.8	487.0

Table 2 show small fluctuations for which some reasons can be given. Firstly, there are inevitable measurement errors which are of an order of magnitude of 1 to 2%.<sup>13</sup> Secondly, there are errors caused by the finite element discretization. By studying the influence of mesh refinement, it was concluded that these are of an order of magnitude of 0.1%. Taking an average value for  $S_u$  from 3P20, 3P40 and 4P40 for material A and from 3P20 and 4P40 for material B it is seen that this average value deviates about 1 to 2% from the individual values given in Table 2. Because of the experimental errors given above, these deviations are considered acceptable. These average values are listed in Table 2 under the column heading Mean and will be used for further analysis. Note that taking the average value as the true value for  $S_u$  strength predictions for the three- and four-point bend tests will deviate about 1 to 2% from the measured values.

#### 4 Biaxial Strength Predictions and Model Verification

Using the value for the unit strength  $S_u$  given in Section 3 strength predictions  $\bar{S}_{nom}^{pred}$  can be made for the biaxial tests carried out. The results of the calculations are listed in Table 3, where the deviations from the measured values  $\bar{S}_{nom}$  are indicated by  $\varepsilon$ :

$$\varepsilon = \frac{\bar{S}_{nom}^{pred} - \bar{S}_{nom}}{\bar{S}_{nom}} \times 100\% \quad (4)$$

Clearly for material A, Wesgo alumina, NSA yields the best prediction while for material B, NKA alumina, GMAX-PSC and RNC-PSC with  $\alpha = 1.1$  yield the best prediction. It is also obvious that the best fitting models for the two materials cannot be interchanged, which indicates a strongly different

**Table 3.** Errors  $\varepsilon$  in the predicted values for the mean fracture stress for materials A and B from the results of biaxial bend tests

Model	Material A: Wesgo		Material B: NKA	
	BOR	ROR	ROR	
PIA	-4.6	+7.0	-2.8	
GMAX	TTC	-24.0	+7.1	-3.1
GMAX	PSC	-28.6	+9.9	-0.1
NSA		-1.4	-0.3	-13.2
COP	TTC	-21.1	+1.9	-9.6
COP	PSC	-29.1	+2.6	-8.3
RNC $\alpha = 1.0$	TTC	-27.0	+4.5	-5.7
	PSC	-33.1	+6.5	-3.1
	$\alpha = 1.1$ TTC	-31.6	+6.0	-3.8
	PSC	-37.1	+8.8	-0.5

fracture mechanism, possibly due to a different microstructure.<sup>4</sup>

#### 5 Looking for Alternative Test Procedures for Model Discrimination

It has been mentioned in the literature that flexure tests may not provide sufficient evidence to discriminate between various fracture criteria, while the Brazilian disk test or torsion tests might do so.<sup>1</sup> From the results given in Section 4 it is obvious that this is not always true, because a clear distinction between some of the models can be made. Especially for the ball-on-ring test some marked differences can be found. The reason for this is fairly simple: in the ball-on-ring test on the lower surface loaded in tension the central part below the ball is most relevant and there an equibiaxial stress state is found such that  $S_2 \approx S_1 > 0$ . On the upper surface not only compressive stresses occur as elementary plate bending theory predicts, but near the edge of the Hertzian contact zone between ball and specimen

simultaneous compressive and tensile stresses occur, as mentioned by Woinowsky-Krieger.<sup>14</sup> These stresses significantly contribute to the value of the stress surface integral. From the results in Table 3 it can be concluded the choice of fracture criterion has a strong influence on the predicted fracture stress, showing the sensitivity of the criteria for mixed tension and compression. The question may then be put forward whether tests in which a major part of the surface is loaded in mixed tension and compression should yield larger differences between the various fracture criteria. To discuss this problem in more general terms equations (2) and (3) are considered. Equation (3) can be reformulated to

$$\Sigma(A) = \frac{1}{A} \int_A \left( \frac{S_1}{S_{\text{nom}}} \right)^m \left[ \frac{1}{2\pi} \int_{C_u} \left( \frac{\sigma_{\text{eq}}}{S_1} \right)^m dC_u \right] dA \quad (5)$$

where  $S_1$  is the largest positive principal stress. Now consider a stress state in which the ratio  $\lambda = S_2/S_1 \leq 1$  is uniform, such that it does not vary within the specimen. Then eqn (5) can be rewritten

$$\Sigma(A) = I(\lambda) \frac{1}{A} \int_A \left( \frac{S_1}{S_{\text{nom}}} \right)^m dA \quad (6)$$

$$I(\lambda) = \frac{1}{2\pi} \int_{C_u} \left( \frac{\sigma_{\text{eq}}}{S_1} \right)^m dC_u \quad (7)$$

For the various fracture criteria considered the value of  $I(\lambda)$  will be different but it will only depend on  $\lambda$ ,  $m$  and possibly Poisson's ratio  $\nu$ , as can readily be deduced from the relations given in Appendix. Note that pure torsion is given by  $\lambda = -1$ , uniaxial tension by  $\lambda = 0$  and equibiaxial flexure by  $\lambda = +1$ . To be able to compare predictions for various models the predicted value for PIA will be taken as an arbitrary but convenient reference. Then the ratio  $R_p$  of the predicted mean fracture stress  $\bar{S}$  for a particular model and the predicted mean fracture stress  $\bar{S}_R$  for PIA can be derived using eqns (2), (6) and (7):

$$R_p = \frac{\bar{S}}{\bar{S}_R} = \frac{S_u}{S_{uR}} \left[ \frac{I_R(\lambda)}{I(\lambda)} \right]^{1/m} \quad (8)$$

with  $S_u$  as the unit strength for the model considered and  $S_{uR}$  as the unit strength for PIA.  $S_u$  and  $S_{uR}$  can be related by requiring that all models predict the same value for uniaxial tension or  $\lambda = 0$  which occurs for three- and four-point bend tests with sufficiently slender specimens. From this condition it results that

$$\frac{S_u}{S_{uR}} = \left[ \frac{I(\lambda=0)}{I_R(\lambda=0)} \right]^{1/m} \quad (9)$$

and

$$R_p = \frac{\bar{S}}{\bar{S}_R} = \left[ \frac{I(\lambda=0)}{I_R(\lambda=0)} \frac{I_R(\lambda)}{I(\lambda)} \right]^{1/m} \quad (10)$$

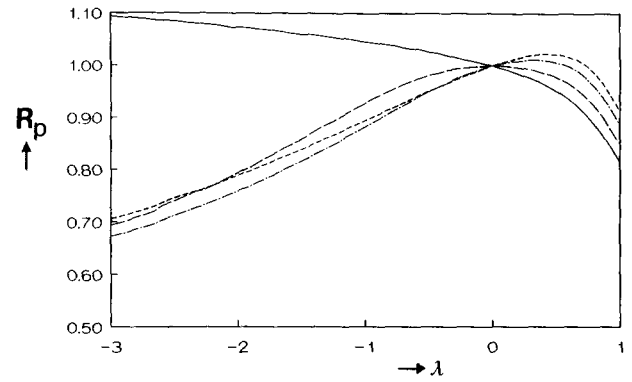


Fig. 1. The ratio  $R_p$  as a function of  $\lambda$  for a Weibull modulus  $m$  of 8 and through-the-thickness cracks (TTC). —, NSA; — — —, COP; ·····, GMAX; - · - · - ·, RNC ( $\alpha = 1.0$ ).

With the equations in the Appendix it is easily found that

$$\begin{aligned} I_R(\lambda) &= (1 + \lambda^m)^{1/m} \text{ if } \lambda \geq 0 \\ I_R(\lambda) &= 1 \text{ if } \lambda < 0 \end{aligned} \quad (11)$$

Without finite element analysis  $R_p$  can easily be evaluated for the various models by numerical integration using the equations given in the Appendix. As an example Figs 1 and 2 give  $R_p$  for GMAX, NSA, COP and RNC with TTC for Weibull moduli of 8 and 22.1. From these figures some conclusions can be drawn. The predicted values for ROR given in Section 4 can be obtained directly from these figures as the ratio  $R_p$  for the various predictions agrees closely to the values in Figs 1 and 2 for  $\lambda \approx 0.9$ . This was to be expected from the beginning as ROR is, to a good approximation, uniformly equibiaxial. Furthermore, it turns out that the predictions for BOR for material A, Wesgo alumina, can be retrieved from Fig. 2 for a value of  $\lambda \approx -1.7$ . This value for  $\lambda$  can be seen as a kind of effective principal stress ratio for the test considered, which does not match the value of 1, which could be expected using elementary plate-bending theory. This supports the remarks made at the beginning of this section with respect to the importance of the

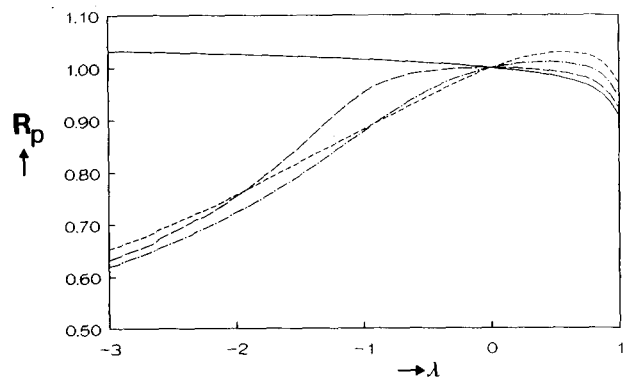


Fig. 2. The ratio  $R_p$  as a function of  $\lambda$  for a Weibull modulus  $m$  of 22.1 and through-the-thickness cracks (TTC). —, NSA; — — —, COP; ·····, GMAX; - · - · - ·, RNC ( $\alpha = 1.0$ ).

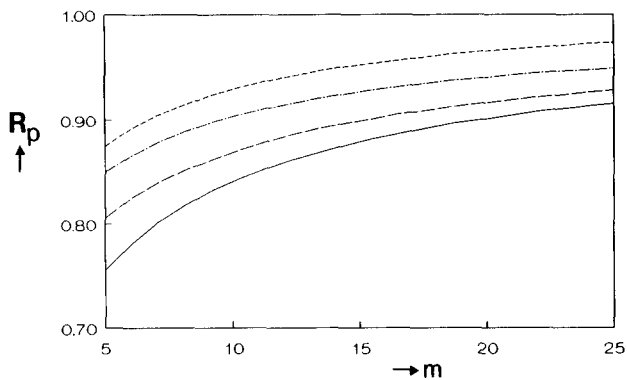


Fig. 3. The ratio  $R_p$  as a function of the Weibull modulus  $m$  for  $\lambda = -1$  and through-the-thickness cracks (TTC). —, NSA; ---, COP; - · - · -, GMAX; · · · · ·, RNC ( $\alpha = 1.0$ ).

occurrence of mixed tension and compression in the ball-on-ring test. Now, other tests could be considered as well. In pure torsion  $\lambda = -1$  and large differences between various fracture criteria might be expected. This turns out to be only partially true. Figures 3 and 4 show that the following remarks can be made:

- In general it will be difficult to discriminate between GMAX and RNC ( $\alpha = 1.0$ ) using the results from a test with an experimental accuracy of 1–2%.
- For  $-3 \leq \lambda \leq -1$  it should be possible to discriminate between PIA and NSA on the one hand and COP, GMAX and RNC on the other.

These and similar conclusions in the case of penny-shaped cracks lead to the conclusion that alternative tests for flexure tests are not necessarily providing additional information and therefore have to be considered with caution. Ideally a combination of several tests with  $\lambda$  varying from negative to +1 should be used to decide whether a particular failure model can be applied. A combination of uniaxial (three- or four-point test) and biaxial (ring-on-ring and ball-on-ring test) results might provide a suitable start.

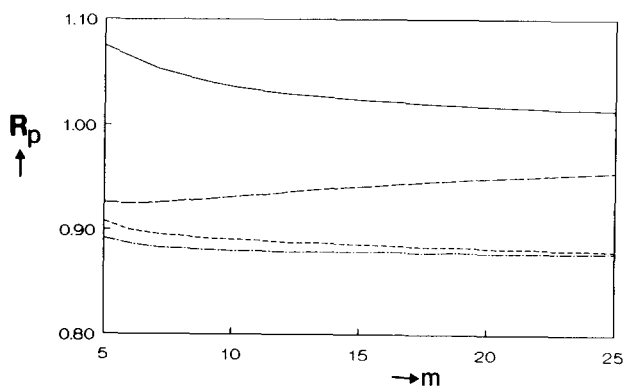


Fig. 4. The ratio  $R_p$  as a function of the Weibull modulus  $m$  for  $\lambda = +1$  and through-the-thickness cracks (TTC). —, NSA; ---, COP; - · - · -, GMAX; · · · · ·, RNC ( $\alpha = 1.0$ ).

## 6 Concluding Remarks

Strength data obtained from uniaxial and biaxial bend tests on two alumina ceramics have been analysed by means of a weakest-link model with different mixed-mode fracture criteria and crack shapes. Taking the data from three- and four-point bend tests as a reference, the model parameters could be determined with a deviation on average matching the experimental accuracy. Using these data, strength predictions for the ball-on-ring and ring-on-ring biaxial tests were made showing large differences in the predictions for the different fracture criteria. The best fitting models for the two aluminas cannot be interchanged, thus showing a marked difference in their shear stress sensitivity. The origin of this shear stress sensitivity is possibly due to their different microstructure. An analysis for homogeneously stresses components has been presented to discuss whether alternative test procedures could yield a better starting point for model discrimination. The conclusion is that, even in the case of mixed tension and compression, differences in the strength predictions for some of the fracture criteria are not large enough with respect to experimental errors. Therefore a combination of test results, e.g. a combination of uniaxial, biaxial with mixed tension and compression and biaxial with tension only, is required to determine which mixed-mode fracture criterion can best be applied. In some cases in metals engineering such an approach is also required, because simply applying the von Mises equivalent stress does not yield reliable results. It is the authors' belief that such a characterization will also be indispensable to validate strength and survival probability predictions for multiaxially loaded ceramics.

## Acknowledgement

This work has partly been supported by the Commission for the Innovative Research Program Technical Ceramics (IOP-TK) of the Ministry of Economic Affairs in The Netherlands (IOP-TK research grant 88.B040).

## References

1. Thiemeier, T., Brückner-Foit, A. & Kölker, H., Influence of the fracture criterium on the failure prediction of ceramics loaded in biaxial flexure. *J. Am. Ceram. Soc.*, **74** (1991) 48–52.
2. Batdorf, S. B. & Crose, J. G., A statistical theory for the

fracture of brittle structures subjected to nonuniform polyaxial stresses. *J. Appl. Mech.*, **41** (1974) 459–61.

3. Batdorf, S. B. & Heinisch, H. L., Weakest-link theory reformulated for arbitrary fracture criterion. *J. Am. Ceram. Soc.*, **61** (1978) 355–8.
4. de Smet, B., Bach, P. W., Dortmans, L. J. M. G., Scholten, H. F. & de With, G., Weakest-link failure prediction for ceramics. Part III: Uniaxial and biaxial bending tests on alumina. *J. Eur. Ceram. Soc.*, **10** (1992) 101–7.
5. Lamon, J. & Evans, A. G., Statistical analysis of bending strengths for brittle solids: A multiaxial fracture problem. *J. Am. Ceram. Soc.*, **66** (1983) 177–82.
6. Nemeth, N. N., Manderscheid, J. M. & Gyenkenyesi, J. P., Design of ceramic components with the NASA/CARES computer program. NASA Technical Memorandum 102369, NASA Lewis Research Center, Cleveland, Ohio, USA, 1990.
7. Evans, A. G., A general approach for the statistical analysis of multiaxial fracture. *J. Am. Ceram. Soc.*, **61** (1978) 302–8.
8. Stanley, P., Fessler, H. & Seville, A. D., An engineers approach to the prediction of failure probability prediction of brittle components. *Proc. Brit. Ceram. Soc.*, **22** (1973) 453–87.
9. Paris, P. C. & Sih, G. C., Stress analysis of cracks. In *Fracture Toughness Testing and Its Applications*, ASTM STP 381. American Society for Testing and Materials, Philadelphia, PA, 1965, pp. 30–83.
10. Hellen, T. K. & Blackburn, W. S., The calculation of stress intensity factors for combined tensile and shear loading. *Int. J. Fract.*, **10** (1974) 305–21.
11. Richard, H. A., Prediction of fracture of cracks subjected to combined tensile and shear loads. VDI Research Report 631/85, VDI, Dusseldorf, Germany, 1985 (in German).
12. Dortmans, L. J. M. G. & de With, G., Weakest-link failure predictions for ceramics using finite element post-processing. *J. Eur. Ceram. Soc.*, **6** (1990) 369–74.
13. Scholten, H. F., Dortmans, L. J. M. G., de With, G., de Smet, B. & Bach, P. W., Weakest-link failure prediction for ceramics II: Design and analysis of uniaxial and biaxial bend tests. *J. Eur. Ceram. Soc.*
14. Woinowsky-Krieger, S., Der Spannungszustand in dicken elastischen Platten. *Ingenieur-Archiv*, **4** (1933) 305–16 (in German).

## Appendix

### Expressions for $\sigma_{eq}$ for the Various Fracture Criteria

Consider a material point on the surface of a component with a stress state characterized by the two principal stresses  $S_1 > S_2$  whose ratio is given by  $\lambda = S_2/S_1$ . Now, in any case,  $\sigma_{eq} = 0$  if  $S_1 < 0$ . A plane

crack, whose orientation with respect to the coordinate system of the principal stresses is given by the angle  $\phi$ , is subjected to a normal stress  $\sigma_n$  and a shear stress  $\tau$  given by

$$\sigma_n = S_1[\cos^2 \phi + \lambda \sin^2 \phi] \quad (A1)$$

$$\tau^2 = S_1^2(1 - \lambda)^2 \sin^2 \phi \cos^2 \phi \quad (A2)$$

Following the lines and formulae given by Thiemeier *et al.*<sup>1</sup> an expression for  $\sigma_{eq}$  for the various fracture criteria used can be given in terms of  $\sigma_n$ ,  $\tau$  and  $\lambda$ .

### NSA: Normal stress averaging or mode I failure

$$\sigma_{eq} = \sigma_n H(\sigma_n)$$

with

$$H(x) = 1 \text{ if } x > 0 \\ = 0 \text{ otherwise}$$

### COP: Coplanar energy release rate

$$\sigma_{eq} = \sqrt{\sigma_n^2 + \mu^2 \tau^2} H(\sigma_n)$$

For through-the-thickness cracks (TTC)  $\mu = 1$ , while for penny-shaped cracks (PSC)  $\mu = 2/(2 - \nu)$ .

### GMAX: Maximum non-coplanar energy release rate

$$\sigma_{eq} = \sqrt[4]{\sigma_n^4 + 6\mu^2 \sigma_n^2 \tau^2 + \mu^4 \tau^4} H(\sigma_n)$$

For through-the-thickness cracks (TTC)  $\mu = 1$ , while for penny-shaped cracks (PSC)  $\mu = 2/(2 - \nu)$ .

### RNC: Empirical criterium of Richard

$$\sigma_{eq} = \frac{1}{2}[\sigma_n + \sqrt{\sigma_n^2 + 4\mu^2 \alpha \tau^2}] H(\sigma_n)$$

For through-the-thickness cracks (TTC)  $\mu = 1$ , while for penny-shaped cracks (PSC)  $\mu = 2/(2 - \nu)$ .  $\alpha$  is a user specified parameter.

### PIA: Principal of independent action

$$\sigma_{eq} = S_1(1 + \langle \lambda \rangle^m)^{1/m}$$

with  $\langle x \rangle = x$  if  $x > 0$   
 $= 0$  otherwise